

1 **Asphalt concrete subjected to long-time loading at low temperatures –**  
2 **deviations from the time-temperature superposition principle**

3 Mariusz Jaczewski, Jozef Judycki, Piotr Jaskuła

4 *Highway and Transportation Engineering Department, Faculty of Civil and*  
5 *Environmental Engineering, Gdansk University of Technology, Gdansk, Poland*

6 Gdansk University of Technology, Faculty of Civil and Environmental Engineering

7 Narutowicza Street 11/12

8 Gdansk, PL 80-233

9 tel.:+48 58 347 27 82

10 e-mail: [mariusz.jaczewski@pg.edu.pl](mailto:mariusz.jaczewski@pg.edu.pl)

11           **Abstract**

12           The article presents the observed deviations from the time-temperature  
13 superposition principle of asphalt concretes, tested in the bending beam creep test at low  
14 temperatures for a long time of loading. In almost all tested asphalt concretes,  
15 deviations appeared after 500 seconds of loading at the temperature of  $-10^{\circ}\text{C}$ . Some  
16 types of bitumen presented deviations at other temperatures – usually the harder the  
17 grade of the bitumen, the higher was the temperature of appearance of deviation. The  
18 article investigates also the impact of the following factors on the described deviations:  
19 type of bitumen, assumed time of loading and level of loading.

20   **Keywords:** low-temperature properties; master curve; viscoelasticity; creep;  
21 deviations from time-temperature superposition principle

## 22        **1. Introduction**

### 23        1.1. Background

24            The time-temperature superposition and thermo-rheological simplicity principles  
25 belong to the basic assumptions in the linear viscoelastic analysis of bitumen and  
26 asphalt mixtures. Since the first applications of these principles for polymers [1] and,  
27 later, bitumen and asphalt mixtures in the 1960s [2], they have been commonly used [3].  
28 The concept of a single curve to describe the behaviour of the tested material for the  
29 whole temperature and time range is very useful. In most cases, especially normalised  
30 test procedures, bitumen and asphalt mixtures comply with the aforementioned  
31 principles. However, in some cases both bitumen and asphalt mixtures show results  
32 different than predicted on the basis of the time-temperature superposition principle. A  
33 few different types of deviations from these principles are known and described in the  
34 literature.

35            In the case of bitumen, deviations from one straight curve may be visible,  
36 especially in the case of bitumen modification with different kinds of polymers [4–11]  
37 or as a results of ageing of the bitumen [12]. These deviations are especially apparent in  
38 the black diagram as separate lines for different temperatures. Some researchers even  
39 describe this kind of behaviour, where it is possible to create one unique curve for  
40 stiffness modulus, but not in the case of phase angle, as “partial time-temperature  
41 superposition principle” [11,13]. Deviations from the thermo-rheological simplicity  
42 were also reported by [14]. Stiffness moduli of the tested bitumen predicted in the  
43 research were slightly higher than those obtained directly from the laboratory tests.

44            In the case of bitumen-filler mastics and asphalt mixtures it is generally accepted  
45 that materials comply with the time-temperature superposition principle and thermo-



46 rheological simplicity. Deviations from those principles are not commonly described.  
47 Nevertheless, some researchers [15–20] reported behaviour which was not completely  
48 consistent with the commonly accepted rheological models. Laboratory tests described  
49 in the mentioned studies were conducted at moderate or elevated temperatures.

50         The authors of this paper observed that for long times of loading at low  
51 temperatures asphalt concretes exhibited evident deviations from thermo-rheological  
52 simplicity. In the creep test conducted on beam specimens, tested asphalt concretes  
53 behaved similarly to solid elastic materials – their creep under constant load either  
54 stopped or strongly decreased. The value of stiffness modulus in some tested cases for a  
55 long loading time was almost constant and it seemed to be independent of the time of  
56 loading. The probable explanation of this case was that the time of loading was still too  
57 short. For long loading times, when the value of stiffness modulus is almost  
58 independent from the time of loading, the validity of the time-temperature superposition  
59 principle is doubtful. While the experimental results obtained at the three tested  
60 temperatures can be shifted and the first parts of the stiffness curves (until around 500  
61 seconds) comply completely with the time-temperature superposition principle, the  
62 values obtained for longer times will not coincide with the rest of the results. They will  
63 usually present either asymptotic behaviour (in the case of hard grade bitumen) or slope  
64 different than the stiffness modulus master curve (in the case of softer bitumen). For  
65 these longer times of loading, values determined from the constructed master curve will  
66 be much lower than those obtained from the laboratory investigation. Moreover, the  
67 deviation from the master curve increases with the increase in the time of loading [21–  
68 23]. This kind of deviation can result in generating large errors in computational  
69 analyses performed on the basis of master curve models, when long times of loading are  
70 taken into consideration [24]. Interestingly, this kind of behaviour was not noted in the

71 long time creep tests conducted on asphalt concretes at higher temperatures [25], even  
72 when laboratory tests were made in the range of strain which strongly exceeded the  
73 assumed limit of linear behaviour.

## 74 1.2. Modelling of asphalt concrete

75 Literature presents numerous models used for description of behaviour of  
76 asphalt concrete under static loading [26], such as series-parallel models, spectral  
77 response functions, ladder models and mathematical models. In this analysis only the  
78 two most commonly used types of models were taken into consideration: series-parallel  
79 Burgers models and different mathematical models of master curves. In further studies  
80 application of 2S2P1D [27] for description of test data is planned.

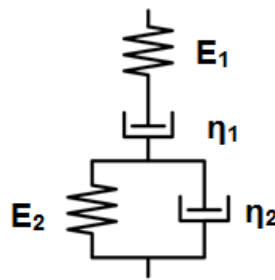
81 It was assumed that materials presented and analysed in this paper can be  
82 modelled as linear-viscoelastic materials, i.e. relation between stress and strain is linear  
83 and material properties are not dependent on the level of load used or deformation of the  
84 tested specimen. Limit of application of linear viscoelasticity is given in the literature in  
85 different approaches: [28–32] suggested that the limit of linear behaviour depends on  
86 the applied stress, the test temperature and time of loading. On the other hand, [5,11,33]  
87 gave the limiting values of strain up to which behaviour of bitumen and asphalt mixture  
88 is assumed as linear. In the case of temperatures below 0°C, the tested asphalt mixture  
89 specimens complied with both of the stated requirements. At the temperature of 0°C the  
90 tested materials exceeded the limit given by Di Benedetto [11], but still presented the  
91 steady flow stage, without any signs of tertiary flow or destruction of the test specimen.

92

93 1.2.1. Series-parallel Burgers model

94 The Burgers series-parallel model, which was used in this paper, is presented in  
 95 Fig. 1. It comprises of 2 dashpots and 2 springs. It is a linear connection of two simple  
 96 viscoelastic models: Maxwell model and Kelvin-Voight model. Despite its simplicity,  
 97 recent research shows that it can be used in prediction of thermal stresses with very  
 98 good reliability [24,34].

99



100  
 101  
 102

Fig. 1. The analysed series-parallel Burgers model.

103 The general stress-strain relationship of the model is given by the following  
 104 differential equation [35]:

$$105 \left[ \frac{d^2}{dt^2} \cdot \frac{\eta_1 \eta_2}{E_1 E_2} + \frac{d}{dt} \left( \frac{\eta_1}{E_1} + \frac{\eta_2}{E_2} + \frac{\eta_1}{E_2} \right) + 1 \right] \cdot \sigma(t) = \left[ \frac{d^2}{dt^2} \frac{\eta_1 \eta_2}{E_2} + \frac{d}{dt} \eta_1 \right] \cdot \varepsilon(t) \quad (1)$$

106 where:  $E_1$  – instantaneous modulus of elasticity, MPa,  $E_2$  – modulus of retarded  
 107 elasticity, MPa,  $\eta_1$  – coefficient of viscosity of steady flow, MPa·s,  $\eta_2$  – coefficient of  
 108 viscosity of retarded flow, MPa·s,  $t$  – time of loading, s.

109 Solution of equation (1) for the case of constant load is given by equation (2).

$$110 \varepsilon(t) = \sigma_0 \left\{ \frac{1}{E_1} + \frac{t}{\eta_1} + \frac{1}{E_2} \left[ 1 - e^{\left(-t/\lambda_2\right)} \right] \right\} \quad (2)$$

111 where:  $\sigma_0$  – constant load, MPa,  $\lambda_2 = \text{retardation time } (\lambda_2 = \eta_2 / E_2), \text{ s.}$

## 112 1.2.2. Master curve mathematical models

113 Assuming that the material complies with the time-temperature superposition  
114 principle and presents linear viscoelastic behaviour, the conception of master curve  
115 enables creation of one line to describe the whole spectrum of temperatures and times of  
116 loading. Master curve is created by shifting separate stiffness curves along the time axis.  
117 The relationship between these curves is described by shift factor  $\alpha_T$ . Master curve  
118 mathematical models used for the description of asphalt concrete are mostly sigmoidal,  
119 sinusoidal or polynomial functions, both symmetrical and nonsymmetrical [26,36].  
120 Every function can be applied with slight modifications for both time and frequency  
121 domains. All of the commonly used master curve functions are phenomenological  
122 equations, which give the best fitting to the available laboratory test data. It is the main  
123 reason why most of them are still subject to corrections and improvements.

124 Shift factor  $\alpha_T$ , which describes relationships between separate stiffness curves  
125 obtained for different temperatures, can be determined using two major approaches –  
126 free shifting or using one of the equations, such as WLF [37][38], logarithmic  
127 polynomial or Kaelble [38].

128 One of the most difficult issues in creation of master curves for asphalt concrete  
129 is the upper stiffness modulus asymptote, due to complex behaviour of the material. In  
130 case of bitumen, limiting value of stiffness modulus is constant and independent of the  
131 used type of bitumen – it ranges from 3 to 6 MPa [4,39]. For asphalt mixtures, either  
132 Witczak [40] or Hirsh [41,42] equations are usually taken into consideration for the  
133 assumption of the maximum modulus. This approach uses basic asphalt mixture



134 properties and maximum value of bitumen stiffness for determination of the modulus.  
 135 However, in the case of asphalt mixtures designed according to the Polish technical  
 136 requirements, results obtained from laboratory tests very often exceeded those  
 137 calculated from mathematical equations, probably due to the use of hard grade bitumen  
 138 (usually 35/50 and even 20/30) in the mixture. In this study, results from laboratory  
 139 tests (ITSM test) conducted at the temperature of  $-30^{\circ}\text{C}$  were assumed as the maximum  
 140 values of stiffness modulus.

141 Two different master curve equations were selected for the study. One of them  
 142 was the CAM model [36,39,43,44], which was originally used for description of  
 143 bitumen behaviour. Its basic function is given by equation (3).

$$144 \quad S(\xi) = S_{\text{glassy}} \left[ 1 + \left( \frac{\xi}{\lambda} \right)^{\beta} \right]^{\frac{\kappa}{\beta}} \quad (3)$$

145 where:  $S_{\text{glassy}}$  – glassy state modulus (maximum stiffness modulus),  $\xi$  –  
 146 reduced time,  $\beta$ ,  $\lambda$ ,  $\kappa$  – fitting parameters.

147 Second model selected for the analysis was the Richards function described in  
 148 [38]. It is a minor modification of the equation used for Simple Performance Test [45].  
 149 Both functions differ by one parameter  $\lambda$ , which changes the equation into a  
 150 nonsymmetrical function. In this study, instead of using Kaelble shift factor, free  
 151 shifting was used to connect stiffness curves obtained at different temperatures.  
 152 Richards model function modified for the purpose of this study is given by:

$$153 \quad \log |E^*| = \delta + \frac{\alpha - \delta}{\left[ 1 + \lambda e^{\beta + \gamma \log(t/t_1)} \right]^{\frac{1}{\lambda}}} \quad (4)$$



154 where:  $|E^*|$  – complex stiffness modulus, psi/MPa,  $t$  – reduced time,  $\delta$  – value of  
155 the lower asymptote (minimum value of stiffness modulus; treated as a fitting  
156 parameter),  $\alpha$  – the value of the upper asymptote (determined from laboratory test  
157 conducted at the temperature of  $-30^\circ\text{C}$ ),  $\lambda$ ,  $\beta$ ,  $\gamma$  – fitting parameters responsible for the  
158 shape of the function.

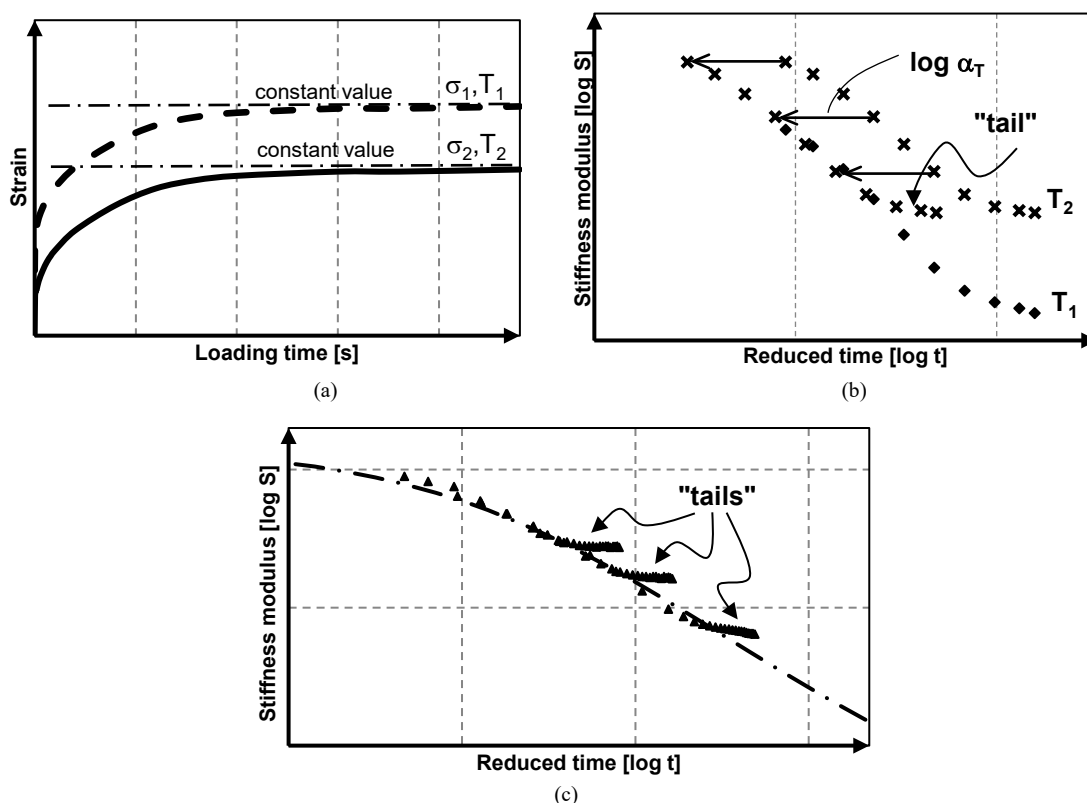
159 In both cases, fitting parameters of the master curve equations were determined  
160 using SOLVER package of MS Excel software. The target function was selected  
161 according to the minimal value of the root mean square error.

## 162 **2. Outline of the deviations from thermo-rheological simplicity**

163 Figs. 2a, 2b and 2c present results typical of an asphalt mix whose behaviour is  
164 inconsistent with the principle of time-temperature superposition. Fig. 2a shows the  
165 creep curve of the mix which, after a long time of constant loading, reaches a constant  
166 (or nearly constant) value of strain or exhibits very slow viscous flow. Such behaviour  
167 is typical of “solid-type” materials and can be described with the Zener model. Most of  
168 the tested asphalt concretes showed such behaviour at low temperatures equal to or less  
169 than  $-10^\circ\text{C}$ . Fig. 2b shows stiffness curves for such materials on a logarithmic scale. It  
170 can be seen that after long loading time the stiffness of the mix reaches a constant value  
171 for a given temperature  $T_1$  or  $T_2$ . After shifting along the time axis, the stiffness curves  
172 at  $T_1$  and  $T_2$  only partly coincide at short time of loading and do not coincide for long  
173 time of loading. Master curve obtained from the shifted stiffness curves is presented in  
174 Fig. 2c. It does not present one smooth curve, but branches into several characteristic  
175 “tails” for each testing temperature below or equal to  $-10^\circ\text{C}$ . The described deviations  
176 from the thermo-rheologically simple behaviour were observed by the authors in most  
177 of the tested materials, regardless of the used mineral mixture or bitumen type. Some

178 exceptions were also observed. First, in the case of hard grade 20/30 neat bitumen,  
 179 where the deviations appeared at the temperature of 0°C. Second, in the case of hard  
 180 grade 20/30 multigrade bitumen, in which the deviations appeared only at the  
 181 temperature of -20°C.

182



183  
184

185  
186  
187  
188

**Fig. 2.** The outline of the deviations from thermo-rheological simplicity: (a) creep curves, (b) stiffness moduli, (c) master curves of stiffness moduli, after [21].

### 189 3. Materials and methods

#### 190 3.1. Materials and preparation

191 Two types of asphalt concretes were used for the purpose of this study – high  
 192 modulus asphalt concrete (HMAC) used for the binder and base course with three types  
 193 of bitumen (neat, polymer modified and multigrade) and, for the sake of comparison, a  
 194 typical asphalt concrete (AC) used for the binder course. Finally, four different mixtures  
 195 were evaluated (AC 16W 35/50; HMAC16 20/30; HMAC16 PMB 25/55-60; HMAC16  
 196 20/30 MG). All of the materials were designed in accordance with the Polish technical

197 requirements and appropriate EN standards. Gneiss aggregate, crushed sand and  
 198 limestone filler were used for the production of the mixtures. No additives were added  
 199 to the asphalt mixtures. Before the compaction of the test specimens, all asphalt  
 200 mixtures were subjected to the procedure of short-term ageing (acc. to SHRP-007  
 201 standard). Basic properties of the bitumen and asphalt mixtures used are presented in  
 202 Tables 1 and 2 respectively. Properties presented in Table 2 were determined during the  
 203 design of the asphalt mixture.

204 **Table 1.** Basic properties of the bitumen used

Property:	Type of bitumen			
	35/50	20/30	PMB 25/55-60	20/30 MG
	neat	neat	SBS-polymer modified	multigrade
Properties before TFOT ageing				
Penetration, 25°C, 0.1 mm, acc. to EN 1426	48	23	28	24
R&B temperature, °C acc. to EN 1427	53	58	62	68
Dynamic viscosity, Pa·s, acc. To EN 12596 at temp.:				
• 60°C	659.3	3063.0	not tested	not tested
• 90°C	15.9	48.5	66.6	137.0
• 135°C	0.6	1.3	1.6	2.0
• 160°C	not tested	0.4	0.5	0.5
Properties after TFOT ageing				
Penetration, 25°C, 0.1 mm, acc. to EN 1426,	45	21	26	24
R&B temperature, °C acc. to EN 1427	57	64	68	72

205  
206

**Table 2.** Basic properties of the asphalt mixtures used

Property	Designation of the asphalt mixture			
	AC 16W 35/50	HMAC16 20/30	HMAC16 PMB 25/55-60	HMAC16 20/30 MG
Grading				
(passes # [mm], %)				
31.5	100	100	100	100
22.4	100	100	100	100
16	97.3	97.8	97.8	97.8
11.2	78.0	81.7	81.7	81.7
8	57.7	62.5	62.5	62.5
5	44.5	49.4	49.4	49.4
2	27.4	32.0	32.0	32.0
0.125	7.1	9.2	9.2	9.2
0.063	5.5	7.3	7.3	7.3
Binder content %, m/m	4.6	5.0	5.0	5.0
Air void content, acc. to EN 12697-8, %	4.3	3.6	3.5	3.5
VMA, %	15.2	15.5	15.4	15.4

VFA, %	71.8	76.9	77.3	77.3
Rutting Resistance, acc. to EN 12697-22, WTS <sub>Air</sub>	0.10	0.10	0.07	0.04
PRD <sub>Air</sub>	6.9	4.8	5.3	4.0

207

208

209

210

211

212

213

214

215

216

217

218

219

220

221

222

223

224

The tests were conducted on beam specimens (50 x 50 x 300 mm). Beam specimens were cut from asphalt mixture slabs (300 x 300 x 50 mm) compacted using a standard Cooper laboratory compactor. The target degree of compaction was determined in the range of 98-100% of Marshall specimen bulk density. Five specimens were cut from each compacted slab.

Preliminary flexural strength test for each test temperature (0°C, -10°C, -20°C) was performed on five beam specimens. The bending beam creep test for each test temperature (0°C, -10°C, -20°C) was performed on at least three specimens. Two remaining specimens from the slab were kept as a reserve for unpredictable situations (for example, if the test machine stopped due to an energy outage). For the entire planned experiment, at least six slabs of each mixture were needed (three for determination of flexural strength and three for bending beam creep test). Before the tests, specimens cut from all the six slabs of a given mixture were mixed and random five beams were chosen for specific test at each temperature. For each beam specimen, air void content was determined, in order to verify whether it was in the range of air void content determined on Marshall specimen.

### 3.2. Methods

225

226

227

228

229

To evaluate the long-time load stiffness modulus, the three point bending beam test (Fig. 3) was used [46,47]. The test was performed in a standard hydraulic press. The test consisted of two phases: in the first phase beams were subjected to constant static load for a time of 2400 seconds; in the second phase beams were left unloaded for a time of 1200 seconds. The applied load depended on the temperature at which the test

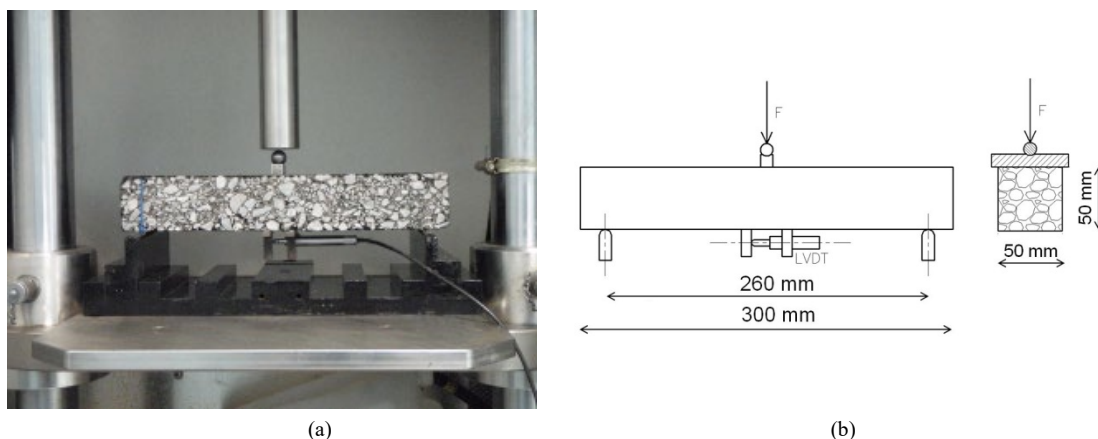
230 was conducted. Load values were assigned as about 30% of the flexural strength. In one  
 231 case (HMAC 20/30), two additional levels of loads were tested. Applied values of load  
 232 are presented in Table 3. Values of applied load vary for different mixtures, depending  
 233 on flexural strength determined in laboratory test. For all beams the test temperatures  
 234 were  $-20^{\circ}\text{C}$ ,  $-10^{\circ}\text{C}$  and  $0^{\circ}\text{C}$ . All specimens were conditioned at the selected  
 235 temperature for 24 hours before the test. The time of conditioning was strictly  
 236 controlled to avoid the influence of physical hardening [48–52] on the values of test  
 237 results. The strain at the bottom of the specimen was measured with an LVDT sensor.  
 238 Coefficient of variation for the measured strain test results equalled up to 20% [46,47].

239 **Table 3.** Applied values of static load

Test temperature	Flexural strength [MPa]	Value of applied stress [MPa]	Value of applied load [kN]
$0^{\circ}\text{C}$	4.17–7.21 (mean 5.80)	1.7–2.2	0.55–0.71
$-10^{\circ}\text{C}$	5.49–7.85 (mean 6.65)	2.7	0.86
$-20^{\circ}\text{C}$	6.02–7.82 (mean 6.75)	2.7	0.86

240

241



242

243

244

245

**Fig. 3.** Bending beam creep test of asphalt concrete: (a) the specimen before the test; (b) scheme of the specimen.

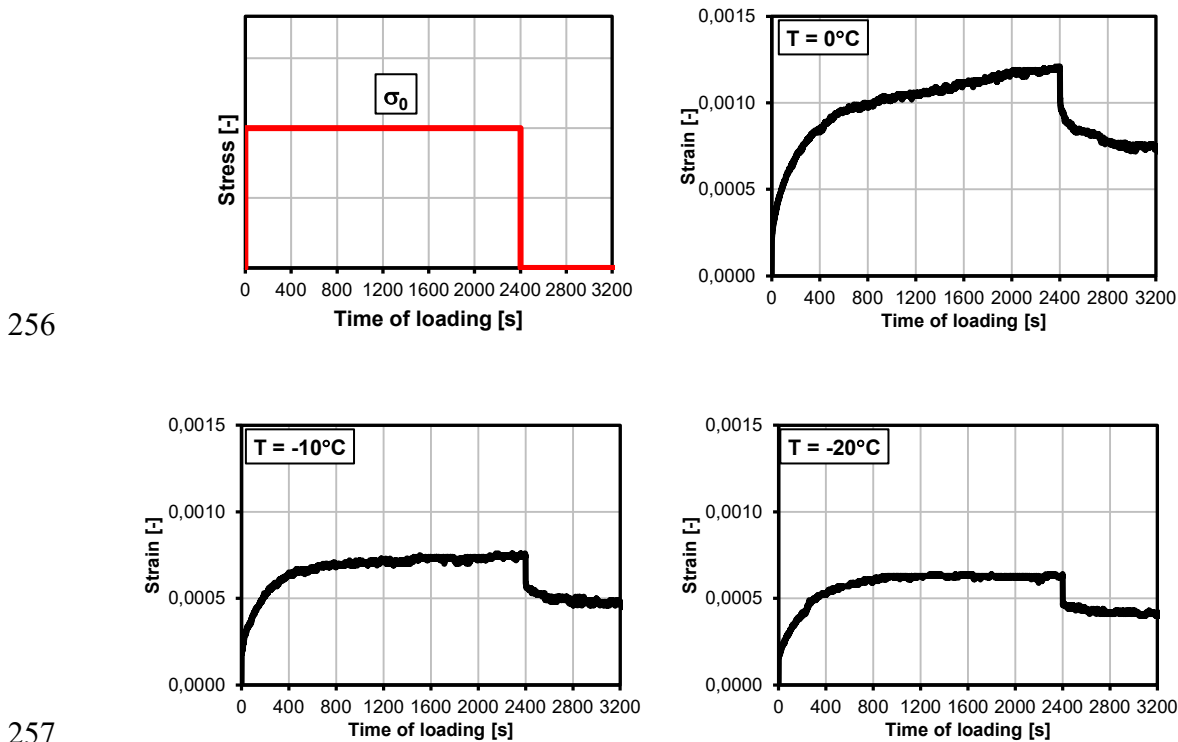
246

## 4. Results and discussion

247

### 4.1. Bending beam creep test results

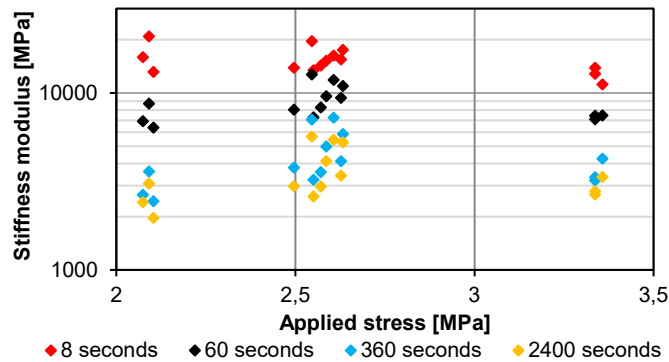
248 Typical creep curves obtained from laboratory tests for the temperatures of 0°C,  
 249 -10°C and -20°C are presented in Fig. 4. The results for each temperature are presented  
 250 for a single specimen from the whole batch of a chosen mixture type. In this case,  
 251 HMAC16 with 20/30 neat bitumen was used as an example. Apart from isolated results  
 252 obtained at the temperature of 0°C, the strain values remained within the linear  
 253 viscoelasticity limit given by Di Benedetto [11]. However, even in the case of the  
 254 temperature of 0°C, when the limit was slightly exceeded, tested specimens showed  
 255 steady flow, without any sign of tertiary flow or specimen destruction.



257  
 258 **Fig. 4.** (a) Applied load; (b), (c), (d) typical creep curves obtained from bending beam creep test of  
 259 asphalt concrete for the temperatures of 0°C, -10°C and -20°C.

260 Additionally, to confirm the assumption of linear viscoelasticity, one mixture –  
 261 HMAC16 with 20/30 neat bitumen – was tested at the temperature of -20°C with three  
 262 different levels of stress. The results for four selected time points (8, 60, 360 and 2400  
 263 seconds) are presented in Fig. 5. Taking into consideration the variability of the test  
 264 results (up to 20% [46,47]), all the results for specific time points, apart from selected

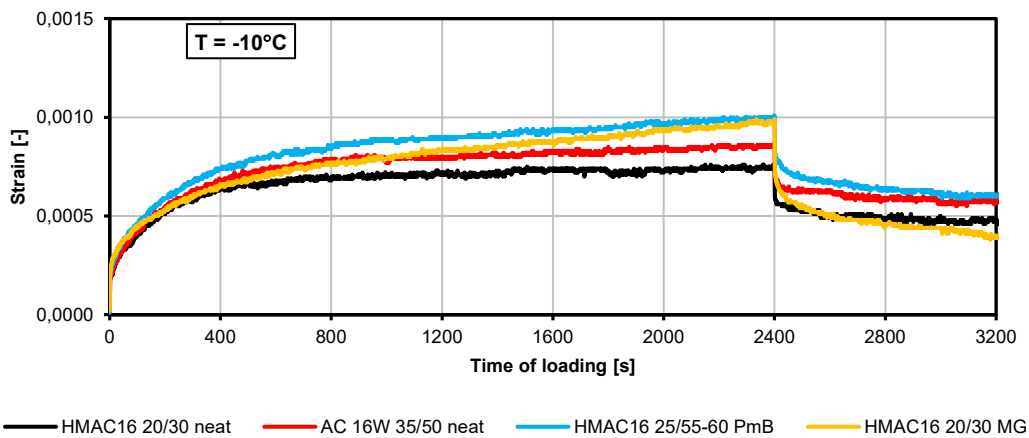
265 results for 8 seconds for the highest applied stress, present similar values of stiffness  
 266 modulus regardless of the stress used.



267

268 **Fig. 5.** Verification of the linear viscoelasticity of tested mixtures. Results for the mixture HMAC16  
 269 with 20/30 neat bitumen, test temperature  $-20^{\circ}\text{C}$ , three levels of applied load.

270 Fig. 6 presents results obtained at the temperature of  $-10^{\circ}\text{C}$  for all the asphalt  
 271 mixtures analysed in this paper.



272

273 **Fig. 6.** Creep curves obtained from the bending beam creep test of asphalt concrete for the  
 274 temperature of  $-10^{\circ}\text{C}$  for all the tested mixtures.

275 As can be seen in Fig. 6, all the tested mixtures comply with Burgers rheological  
 276 model, with all its phases: instant elastic strain and steady creep state for the loaded  
 277 phase, and instant return and steady relaxation during the unloaded phase. All the tested  
 278 mixtures present steady creep with time of loading. In the case of hard grade neat  
 279 bitumen (20/30 neat bitumen, black line), it might seem that the steady flow stage of the

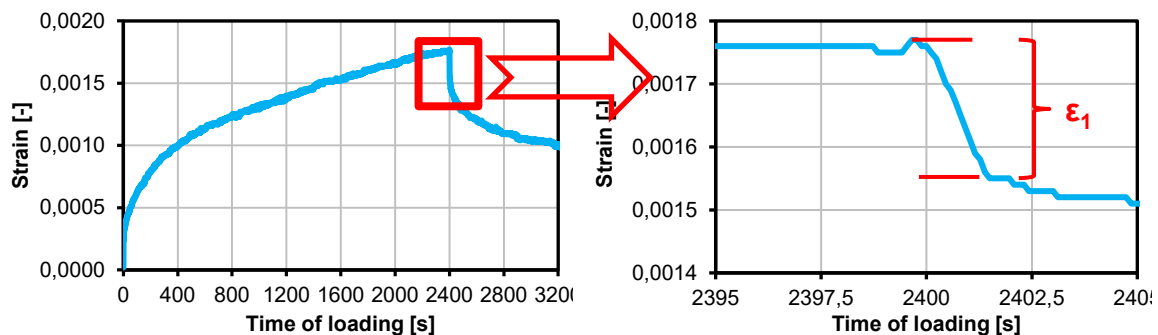
280 creep curve flattens and almost reaches horizontal asymptote. An elongated test, which  
281 lasted 8 hours, showed that the specimen still creeps, but the rate of creep is very slow,  
282 similar to the rate typical of elastic materials, such as cement concrete.

#### 283 4.2. Modelling of asphalt concrete using laboratory test results

284 Test results obtained from the bending beam creep test were later described  
285 using two groups of mathematical models: rheological series-parallel model and master  
286 curve mathematical models using procedures developed at the Department of Highway  
287 Engineering of the Gdansk University of Technology. In all cases the fitting was  
288 performed on the basis of root mean square error criterion.

##### 289 4.2.1. Modelling using rheological series-parallel model

290 Modelling using rheological model was based on the fitting of equation (2)  
291 using root mean square error. Three of the four Burgers model parameters were treated  
292 as fitting parameters:  $E_2$ ,  $\eta_1$  and  $\eta_2$ . In the case of the  $E_1$  elastic modulus, it was  
293 obtained from the unloaded phase of the creep curve, as seen in Fig. 7.  $E_1$  elastic  
294 modulus was calculated as  $E_1 = \varepsilon_1 / \sigma_0$ .

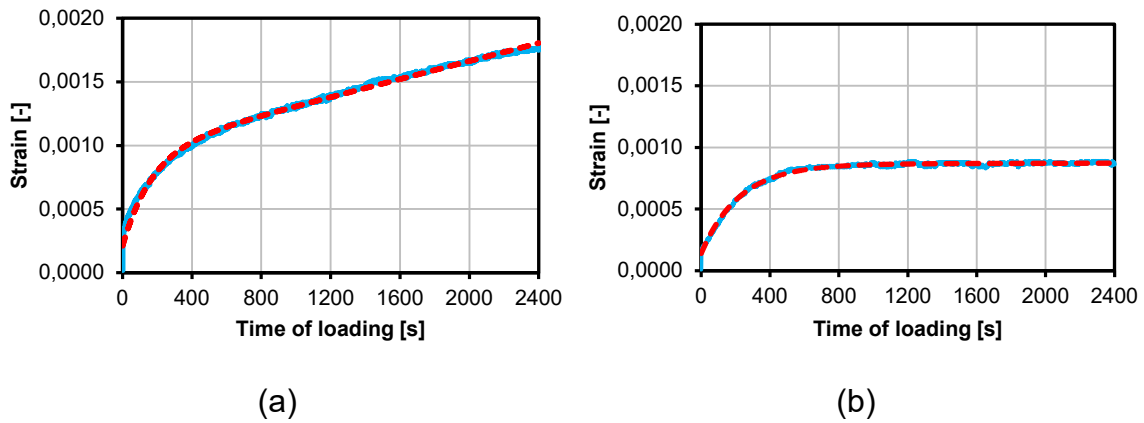


295 **Fig. 7.** Determination of the  $E_1$  elastic modulus of Burgers model.

296 Such a way of calculation of the  $E_1$  parameter resulted in higher homogeneity of  
297 the obtained results and eliminated random deviations coming from the factors



298 associated with the loading phase (especially from the fitting of steel beam used for  
 299 centring of the load on the specimen). Fitting of the test results for different  
 300 temperatures using described methodology is presented in Fig. 8. The determined  
 301 parameters of Burgers model for all the tested asphalt mixtures are presented in Table 4.  
 302



303 **Fig. 8.** Fitting of the creep curves using Burgers model: (a) temperature of 0°C, (b) temperature of  
 304 -20°C (continuous line – experimental results, dashed line – fitting using Burgers model).  
 305

306 **Table 4.** Burgers model parameters for all the tested mixtures

Asphalt mixture	Temperature °C	Burgers model rheological parameters			
		E <sub>1</sub> MPa	E <sub>2</sub> MPa	η <sub>1</sub> MPa·s	η <sub>2</sub> MPa·s
HMAC16 20/30	0	11 666	1 811	19 303 852	327 299
	-10	16 338	4 437	128 667 390	1 000 705
	-20	20 243	7 950	261 050 362	1 801 012
HMAC16 PMB 25/55-60	0	8 107	1 989	4 512 138	434 479
	-10	13 417	4 017	32 637 170	798 762
	-20	17 514	4 331	98 703 764	890 505
HMAC16 20/30 MG	0	4 966	2 423	3 201 052	444 497
	-10	7 048	5 520	8 699 462	1 097 785
	-20	14 328	7 138	194 646 646	1 850 407
AC 16W 35/50	0	7 891	1 469	5 646 589	325 605
	-10	15 609	3 901	55 355 791	783 953
	-20	17 241	4 761	91 268 648	933 607

307 As can be seen in Fig. 6, the obtained creep curves are consistent with the  
 308 Burgers rheological model and the obtained values are similar to those observed in other  
 309 creep tests conducted for asphalt mixtures [46,53,54]. Nevertheless, some discrepancies  
 310 are visible in comparison to the parameters obtained from cyclic tests, such as Simple  
 311 Performance Tester. While both elastic moduli are quite similar, the biggest  
 312 discrepancies are visible in the case of the η<sub>1</sub> parameter – coefficient of viscosity of

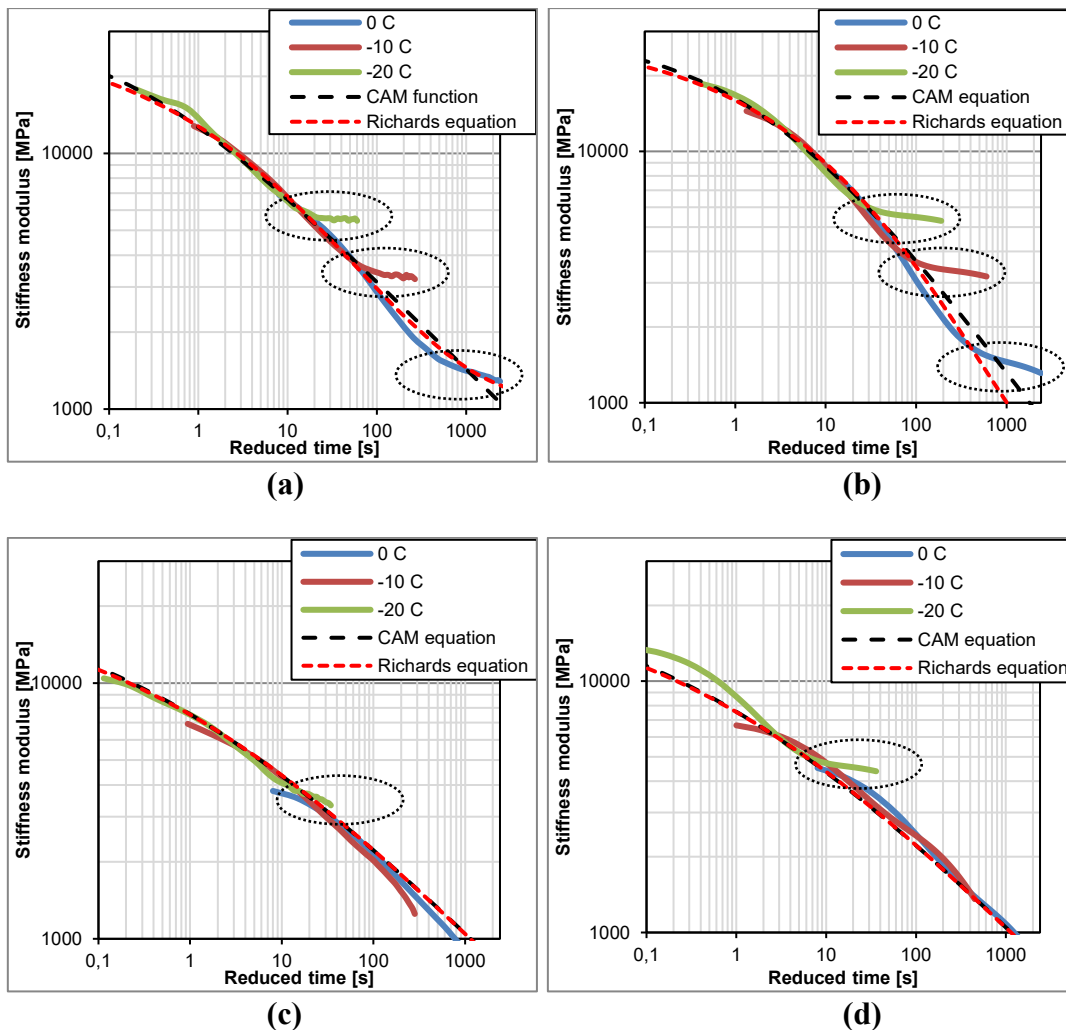
313 steady flow. Results determined from cyclic tests [55–57] differ up to three orders of  
314 magnitude from the results obtained from creep tests. The reason for this discrepancy is  
315 still under research. Nevertheless, Burgers model parameters determined in this study  
316 were recently successfully used for calculation of thermal stresses in [24].

#### 317 4.2.2. Modelling using master curves

318 Master curves were determined using the authors' modifications of the  
319 procedures used for Bending Beam Rheometer (BBR) and its later variant for testing of  
320 asphalt concrete [58–61]. In comparison to the aforementioned studies, the time of  
321 loading was extended to 2400 seconds, instead of typical 1000 seconds. Master curves  
322 were obtained on the basis of free shift of specific stiffness curves determined for the  
323 temperatures of 0°C, –10°C  
324 and –20°C. The temperature of 0°C was selected as the reference temperature. Each  
325 stiffness curve is the mean value of 3 different stiffness curves obtained from each  
326 tested specimen for a selected temperature. Each obtained master curve was later  
327 described using CAM and Richards models, under assumption that results comply with  
328 the thermo-rheological simplicity principle. During construction of the master curve, the  
329 observed deviations were not taken into consideration so as not to influence the shifting,  
330 and data points only up to 500 seconds were utilized. Master curves were constructed on  
331 the basis of results directly from the creep test, but also, separately, from the results  
332 back-calculated from rheological model parameters. The developed master curves,  
333 obtained from both direct and back-calculated results, along with mathematical  
334 description using CAM and modified Richards equations are presented in Fig. 9.

335





336  
337  
338

339  
340  
341  
342  
343

**Fig. 9.** Shifted stiffness curves (free shifting): (a), (c) direct results from the bending beam creep test; (b), (d) results back-calculated from the Burgers model. Deviations from the master curves are highlighted with ovals. Mixtures used: (a), (b) HMAC 20/30; (c), (d) HMAC 20/30 MG.

344

345

346

347

348

349

350

351

352

As can be seen in Fig. 9, for both types of data (directly from the creep test and back-calculated from the Burgers model) master curves obtained after free shifting are very similar. Nevertheless, in all cases, there are visible deviations from one continuous curve. In Fig. 9, two extreme cases are presented. In case of HMAC with 20/30 neat bitumen (Figs. 9a, 9b), horizontal deviation is visible at all the tested temperatures (from 0°C down to -20°C). In the case of HMAC with 20/30 MG, the horizontal deviation appeared only at the temperature of -20°C. In other tested cases – conventional AC and HMAC with polymer modified bitumen – the horizontal deviation appeared at the temperature of -10°C and lower.

353 Parameters of master curves (CAM and Richards models) of all the tested  
 354 materials are presented in Table 5.

355 **Table 5.** Master curve model parameters for all the tested mixtures

Asphalt mixture	Parameters of model				
CAM model					
	$E_{max}$ [MPa]	$\lambda$	$\beta$	$\kappa$	
HMAC 20/30	29 723	0.168	0.506	0.348	
HMAC 25/55-60	27 018	0.203	0.587	0.360	
HMAC 20/30 MG	22 799	0.399	0.283	0.376	
AC 16W 35/50	29 885	0.044	0.857	0.332	
Richards model					
	Max	$\delta^a)$	$\lambda$	$\beta$	$\gamma$
HMAC 20/30	4.473	3.027	0.001	-9.095	-0.696
HMAC 25/55-60	4.431	0.000	5.934	-0.443	-0.826
HMAC 20/30 MG	4.358	0.038	3.760	-0.582	-0.564
AC 16W 35/50	4.475	0.000	8.726	0.463	-0.980

356 Remarks: a)  $\delta$  parameter is responsible for the lower asymptote of the master curve. As can be seen  
 357 from the values presented in tables, for a very long time of loading the stiffness modulus will be  
 358 approaching the value of 0 MPa. While in the case of beam specimens subjected to bending this kind of  
 359 situation is possible (it would be equivalent to the destruction of the specimen), from the physical point  
 360 of view it is an impossibility. Therefore, values presented in the table are in this case treated as fitting  
 361 parameters for the best description of the model at temperatures below 0°C and not as a physically  
 362 sound general description of material's behaviour across the full spectrum of times and temperatures.

363 4.3. Discussion of test results

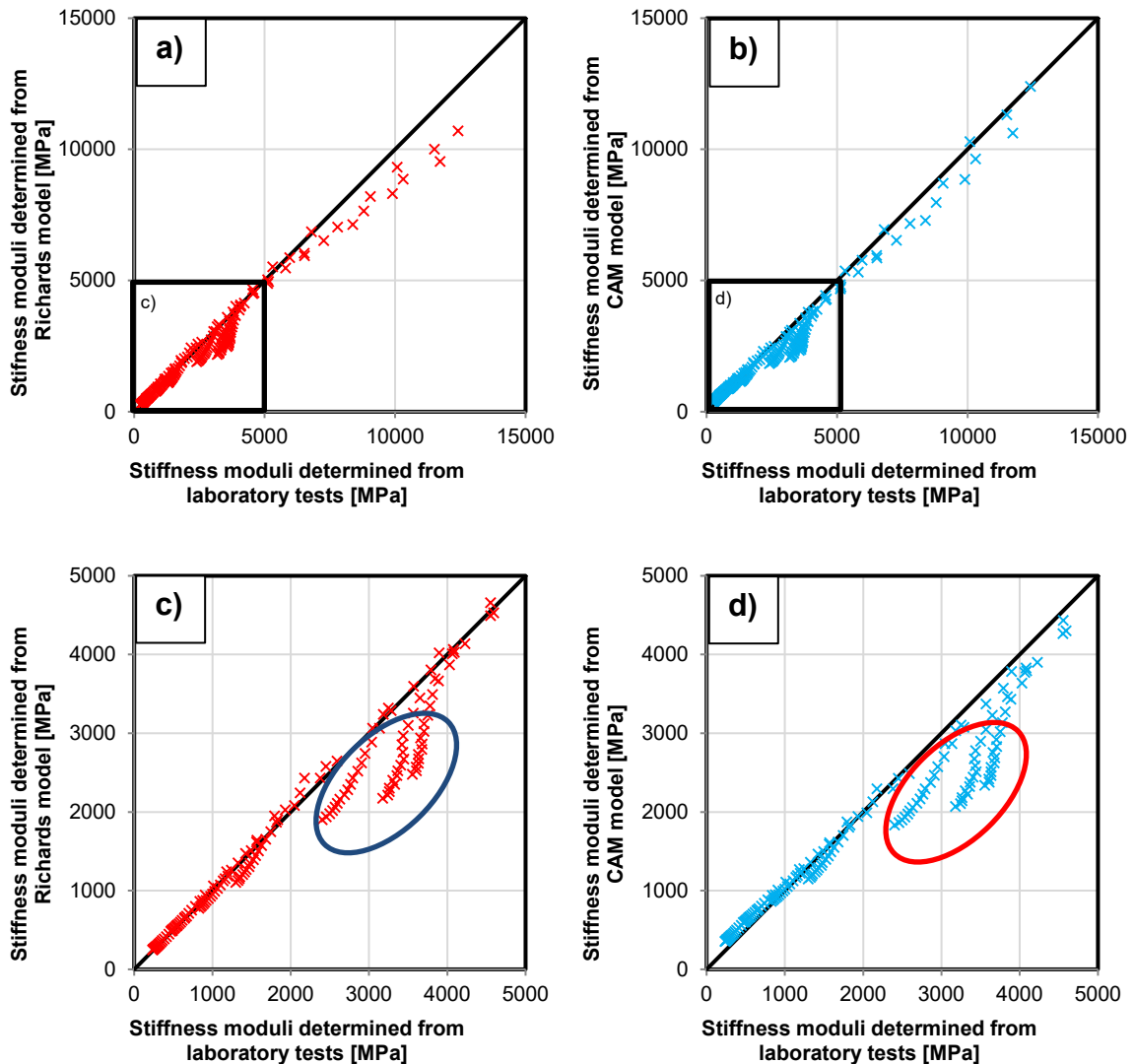
364 As can be seen in Fig. 8, both models gave very similar results, with similar  
 365 fitting quality. Nevertheless, there are two main visible differences:

- 366 • in the case of very short reduced times, Richards model gives values lower than  
 367 those obtained from the laboratory test;
- 368 • in the case of HMAC with 20/30 neat bitumen, CAM model (in contrast to  
 369 Richards model), does not give any opportunity to describe the deviation from  
 370 the straight section of the master curve line, as visible near the 1000s reduced  
 371 time.

372 In one case it was also observed that for very long reduced times CAM model  
 373 gave values higher than those obtained from laboratory tests. Regardless of the used  
 374 model, for temperatures lower than 0°C and long times of loading, values obtained from

375 the models are much lower than values determined from laboratory test. This situation  
376 is presented in Figs. 10b and 10d.

377



378 Remark: in figures c) and d) values obtained from both master curve models that were lower in  
379 comparison to laboratory test data are highlighted with an oval

380  
381  
382

**Fig. 10.** The correctness of the modelling of laboratory test data (HMAC 20/30) using two master curve models: a), c) Richards model; b), d) CAM model.

383 Both of the used master curve models gave similar and very good fitting of the  
384 test data, but only in the case of assumption that tested materials are thermo-  
385 rheologically simple and comply with time-temperature superposition, and time of  
386 loading used for determination of the master curve was reduced to 1000 seconds. This  
387 kind of assumption will give correct results when short-time load phenomena are

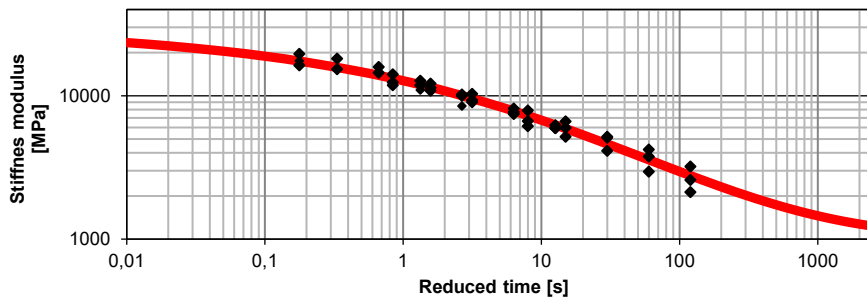
388 modelled. In the case of long-time load phenomena, such as development of thermal  
389 stresses in asphalt pavements, values determined from the master curve will be much  
390 lower and will have strong impact on computational analyses. For example, thermal  
391 stresses calculated using that kind of data will present much lower values than those  
392 measured in the field or in the laboratory.

393 Authors tried to determine the main aspect which influences the appearance of  
394 the described deviations from the models used. At this stage of the research, influence  
395 of the assumed time of loading, type of bitumen and asphalt mixture composition were  
396 taken into consideration.

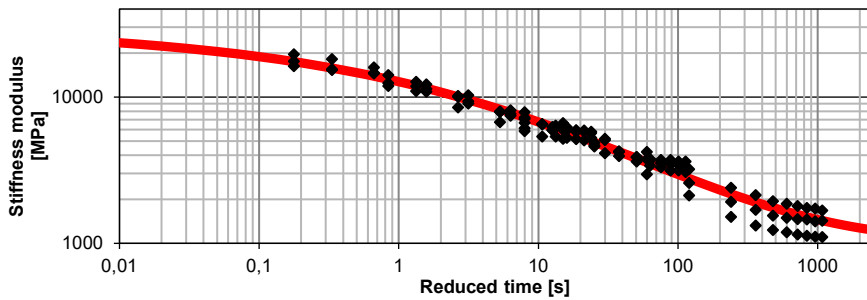
#### 397 4.3.1. The impact of the assumed time of loading on modelling of asphalt concrete

398 As stated above, deviations from the models used appear at temperatures below  
399 0°C, when the time of loading is long, usually after around 500 seconds of loading. On  
400 the other hand, typical laboratory creep test methods assume the maximum time of  
401 loading in the range from 100 to 1000 seconds [58,62,63]. As shown in Fig. 11, even  
402 when the time of loading is assumed as 1000 seconds, the deviations do not have strong  
403 impact on development of the master curve. The problem intensifies when the time of  
404 loading increases above 1000 seconds. The longer the time of loading, the more  
405 noticeable the deviations that appear. This fact is very important when master curve  
406 mathematical models are used for calculation of low temperature processes, such as  
407 thermal stresses induced in real pavements, where very long times of loading are  
408 needed, sometimes exceeding 10000 seconds. In such a case, shifted stiffness curves  
409 would be branching into multiple separate curves.

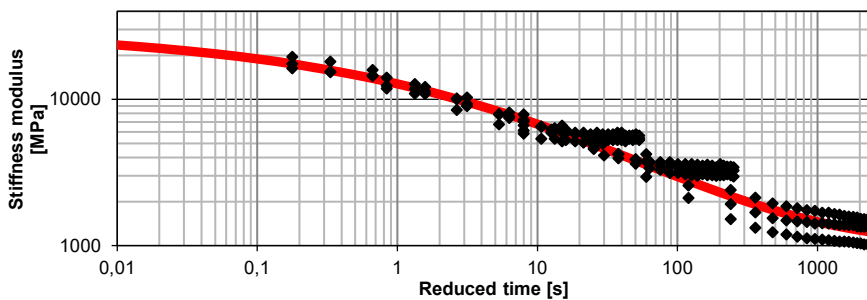
410



(a)



(b)



(c)

411 **Fig. 11.** The influence of time of loading on modelling of the master curve: a) 100 seconds; b) 1000  
412 seconds; c) 2400 seconds.

413 In the case of temperatures higher than  $0^{\circ}\text{C}$ , deviations from the models used  
414 were not observed, even for times of loading equal to 2400 seconds. At lower  
415 temperatures, the appearance of deviation is strongly connected to the assumed time of  
416 loading. In the case of 100 seconds or even 1000 seconds, after appropriate shifting,  
417 deviations do not influence the creation of master curve. “Branching problem” appears  
418 after around 500 seconds of loading and its impact is strongly visible after 1000 seconds

419 of loading. The type of bitumen or type of asphalt mixture did not have strong impact  
420 on the time when the “branching” of the master curve occurred.

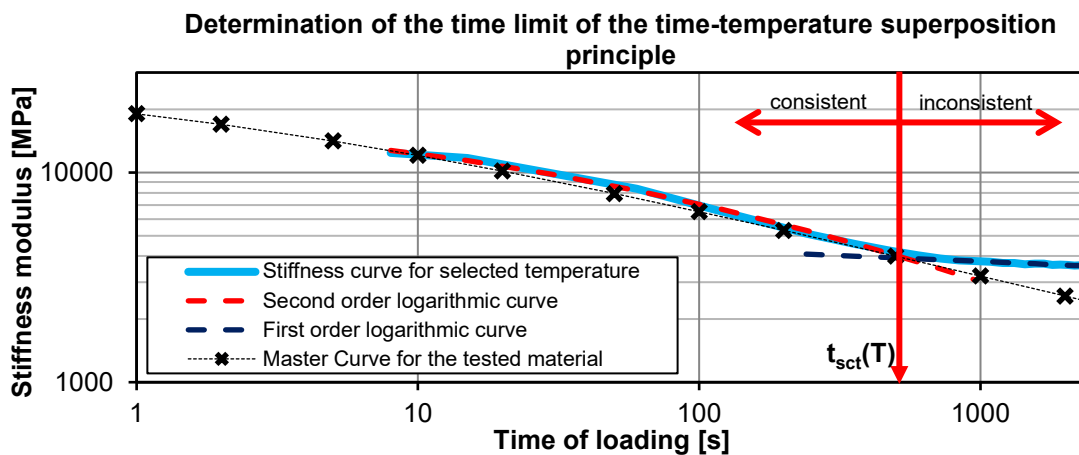
#### 421 4.3.2. Determination of the limit of the time-temperature superposition principle

422 To determine the time limit of application of the time-temperature superposition  
423 principle in analysis of creep test data, each of the stiffness curves was described using  
424 two logarithmic functions (see Fig. 12):

- 425 • Second order curve – for the time range from 0 to around 500 seconds, (based  
426 on an assumption that within this range the stiffness curve is mostly consistent  
427 with the time-temperature superposition principle); this part of the curve  
428 overlaps with the developed master curve for the analysed asphalt mixture.
- 429 • First order curve – for the time range in which the stiffness curve does not  
430 comply with the time-temperature superposition principle. In most cases this  
431 part of the curve approaches the horizontal asymptote.

432 The intersection of the two aforementioned logarithmic curves was assumed to  
433 be the time limit of the time-temperature superposition principle. Determined times  
434 (rounded up to full 20 seconds) of all the tested materials are presented in Table 6.

435



436  
437

Fig. 12. Method used for determination of the limit of the time-temperature superposition principle



438  
439  
440

**Table 6.** The determined limit loading times in which tested materials comply with the time-temperature superposition principle

Temperature [°C]	HMAC 20/30	HMAC 25/55-60	HMAC 20/30 MG	AC 16W 35/50	AC 16W 50/70
-20	520	520	580	460	500
-10	600	440	- <sup>a)</sup>	580	460
0	420	- <sup>a)</sup>	- <sup>a)</sup>	- <sup>a)</sup>	- <sup>a)</sup>

441  
442

a) tested specimens did not show deviation from the time-temperature superposition principle up to 2400 seconds

443

444

445

446

447

Time limit up to which test results were consistent with the time-temperature superposition principle at the temperature of  $-10^{\circ}\text{C}$  and lower lies within the range from 400 to 600 seconds. In the described cases, master curve model covered only around 20-25% of the whole time range of the test, which is not enough for proper material description in terms of low temperature impact on asphalt mixtures.

448

#### 4.3.3. The impact of type of asphalt mixture and bitumen used in asphalt concrete

449

450

451

452

453

454

Apart from the research presented in this paper, similar bending beam creep tests were conducted under other research projects carried out at the Gdansk University of Technology. Regardless of the used type of test machine or asphalt mixture [47,64] – asphalt concrete, high modulus asphalt concrete, stone matrix asphalt, porous asphalt – in all the tested cases at temperatures lower than  $0^{\circ}\text{C}$  deviations appeared after a time of loading longer than approx. 500 seconds.

455

456

457

458

459

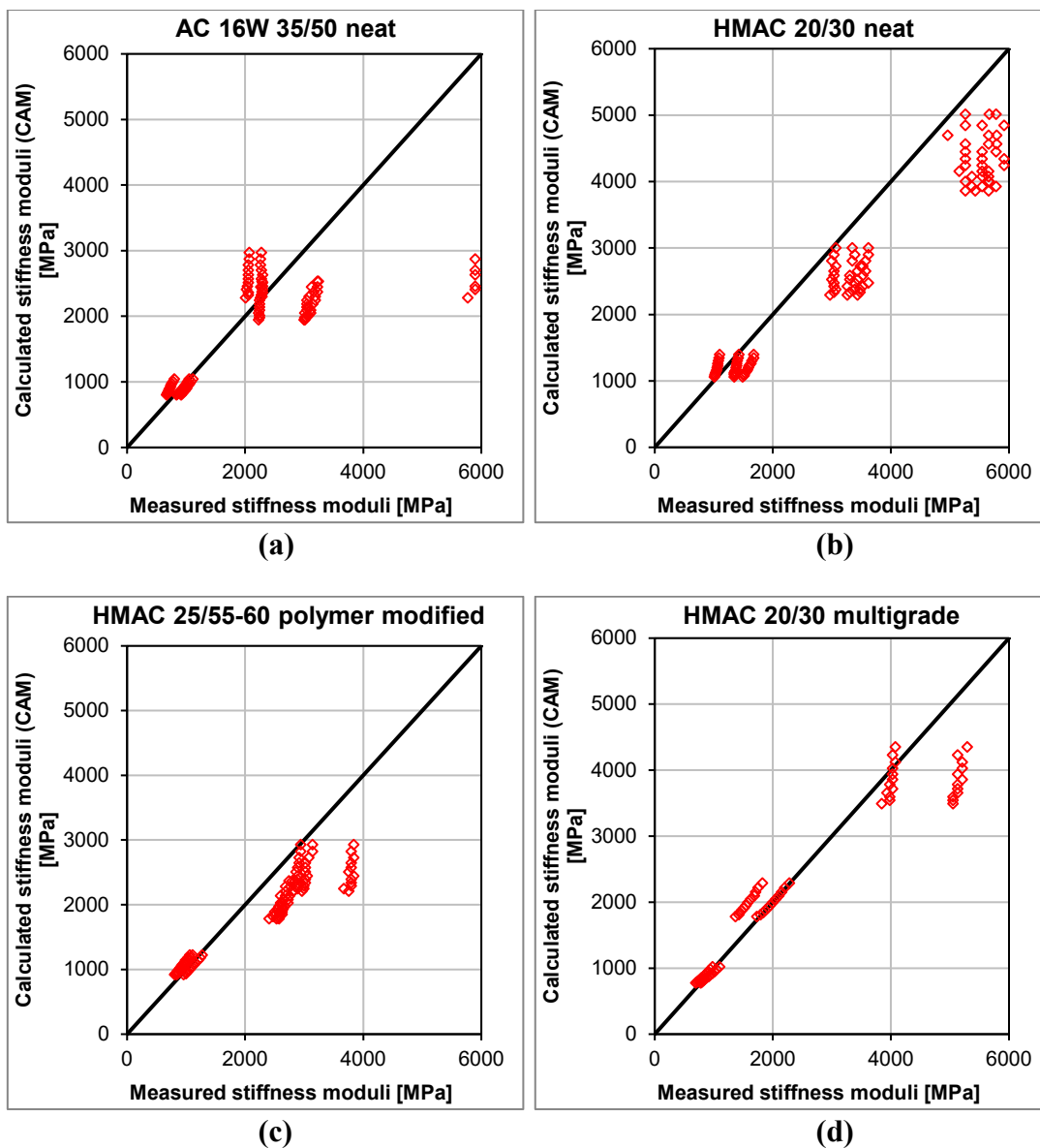
460

461

It was noted that the particular type and grade of bitumen used in the asphalt mixture had a relatively strong impact on the moment of appearance of the deviations. In most cases, the first deviations appeared at the temperature of  $-10^{\circ}\text{C}$ , regardless if neat or polymer modified bitumen was used. Some discrepancies were observed for two types of hard grade bitumen. First, in the case of neat hard grade 20/30 bitumen, the deviation appeared at the temperature of  $0^{\circ}\text{C}$ . This type of bitumen is characterized by a relatively high viscosity even at higher temperatures, which probably resulted in faster

462 “stiffening” of the tested asphalt mixtures. Second case was the hard grade multigrade  
 463 bitumen. In this instance, the deviation appeared much later, at the temperature of  
 464  $-20^{\circ}\text{C}$ . The latter phenomenon, however, cannot be explained by the values of  
 465 viscosity, as the results are similar to the values obtained for a typical polymer-modified  
 466 bitumen. A probable explanation is that the viscoelastic temperature range of this type  
 467 of bitumen is wider, and its behaviour is close to viscoelastic even at the temperature  
 468 near  $0^{\circ}\text{C}$ . All cases are presented in Fig. 13.

469  
 470  
 471



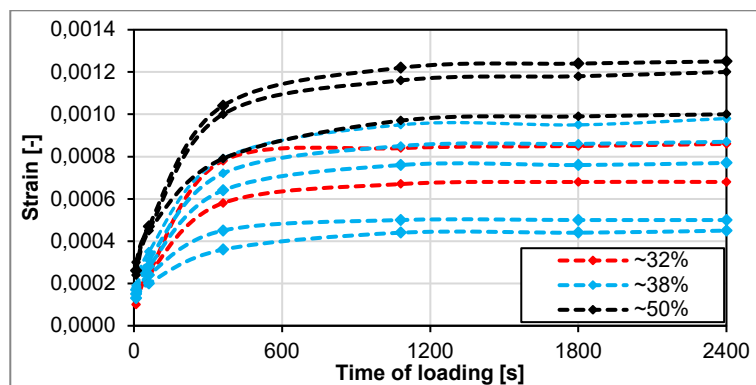
472  
 473  
 474  
 475  
 476  
 477

**Fig. 13.** Differences between calculated and measured stiffness moduli for times of loading longer than 1000 seconds: (a) AC 16W 35/50 neat bitumen, (b) HMAC 20/30 neat bitumen, (c) HMAC 25/55-60 polymer modified bitumen, (d) HMAC 20/30 multigrade bitumen.

478 4.3.4. The impact of the level of static loading

479 In most cases the value of around 30% of flexural strength was used as the  
480 constant stress that the specimen was subjected to. It was worthwhile to analyse whether  
481 the applied stress was too small to induce viscous flow. Tests with higher static load (up  
482 to 50% of flexural strength) were conducted to examine such possibility in additional  
483 research. Results of these tests are presented in Fig. 14. Creep curves measured under  
484 three static load levels (32%, 38% and 50% of flexural strength) show different limits of  
485 strain at long time of loading. For each load level two to five specimens were used.  
486 Limit of strain for static load of 50% of flexural strength is higher than for lower static  
487 loads – 32% and 38% of flexural strength – but it also reaches constant value after time  
488 of loading of about 600 to 1000 seconds. In the case of the two lower static load levels,  
489 the results of the test overlap with each other. This preliminary study on one mixture at  
490 one temperature showed that the time at which strain reaches constant limit depends on  
491 the load level and increases with higher levels of static load. A detailed investigation on  
492 different load levels at different temperatures is planned in further analyses.

493



494  
495  
496

**Fig. 14.** Impact of different levels of static load on behaviour of asphalt mix at creep (creep curves for HMAC 20/30 neat bitumen at the temperature of  $-20^{\circ}\text{C}$ ), after [21] and supplemented.

497 **5. Conclusions and further studies**

498 The described deviations from the material models used can have strong impact  
499 on computational analyses conducted on the basis of master curves. Values of stiffness  
500 modulus determined from master curves for long times of loading are significantly  
501 lowered in comparison to the real values determined from laboratory tests. For example,  
502 in the case of calculation of thermal stresses, the calculated values can be significantly  
503 lowered or even unacceptably underestimated if only the thermo-rheologically simple  
504 part of master curve is taken into consideration. Based on the analysis, the following  
505 conclusions can be made:

- 506 • Series-parallel rheological models described each of the tested materials  
507 correctly at every tested temperature. Burgers model did not present any  
508 problems during modelling of the test data. Correctness of the data was  
509 confirmed in other studies [24].
- 510 • Neither of the master curve models described the tested materials correctly. The  
511 deviations were visible in the case of long times of loading. Under assumption  
512 of short time of loading, laboratory test data allowed to create master curves  
513 without any problems.
- 514 • It was determined that the time-temperature superposition principle limit lied  
515 within the range from 420 to 600 seconds.
- 516 • The appearance of the described deviations depended strongly on the type of  
517 bitumen used (production process and grade). The type of asphalt mixture used  
518 did not influence the appearance of the deviations.



- 519       • The level of static loading does not have strong impact on the occurrence of  
520       deviations from thermo-rheological simplicity. For the higher levels of loading  
521       the time limit of thermo-rheological simplicity principle is slightly higher.
- 522       • “Branching” model of the master curve should be created to model the complex  
523       behaviour of asphalt mixtures at low temperatures for long times of loading.

## 524   **Acknowledgement**

525   It is gratefully acknowledged that the presented research was performed under a  
526   research project sponsored by the Polish General Directorate for National Roads and  
527   Motorways.

## 528   **References**

- 529   [1]   J.D. Ferry, *Viscoelastic Properties of Polymers*, 3rd Edition, 1980.
- 530   [2]   C.L. Monismith, R.L. Alexander, K.E. Secor, *Rheologic Behavior of Asphalt*  
531       *Concrete*, *J. Assoc. Asph. Paving Technol.* 35 (1966) 400–450.
- 532   [3]   Y.R. Kim, *Modeling of Asphalt Concrete*, American Society of Civil Engineers,  
533       2009.
- 534   [4]   G.D. Airey, *Use of Black Diagrams to Identify Inconsistencies in Rheological*  
535       *Data*, *Road Mater. Pavement Des.* 3 (2002) 403–424.
- 536   [5]   G. Airey, *Rheological properties of styrene butadiene styrene polymer modified*  
537       *road bitumens*\*, *Fuel.* 82 (2003) 1709–1719. doi:10.1016/S0016-2361(03)00146-  
538       7.
- 539   [6]   H. Di Benedetto, F. Olard, C. Sauzéat, B. Delaporte, *Linear viscoelastic*

- 540 behaviour of bituminous materials: From binders to mixes, *Road Mater.*  
541 *Pavement Des.* 5 (2004) 163–202. doi:10.1080/14680629.2004.9689992.
- 542 [7] G.D. Airey, M.H. Mohammed, Rheological properties of polyacrylates used as  
543 synthetic road binders, *Rheol. Acta.* 47 (2008) 751–763. doi:10.1007/s00397-  
544 007-0250-3.
- 545 [8] G. Airey, M. Mohammed, A.C. Collop, C.J. Hayes, T. Parry, Linear Viscoelastic  
546 Behaviour of Polyacrylate Binders and Bitumen Blends, *Road Mater. Pavement*  
547 *Des.* 9 (2008) 13–35. doi:10.1080/14680629.2008.9690157.
- 548 [9] N.I.M. Yusoff, E. Chailleux, G.D. Airey, A Comparative Study of the Influence  
549 of Shift Factor Equations on Master Curve Construction, *Int. J. Pavement Res.*  
550 *Technol.* 4 (2011) 324–336.
- 551 [10] E. Santagata, O. Baglieri, L. Tsantilis, D. Dalmazzo, Rheological  
552 Characterization of Bituminous Binders Modified with Carbon Nanotubes,  
553 *Procedia - Soc. Behav. Sci.* 53 (2012) 546–555.  
554 doi:10.1016/j.sbspro.2012.09.905.
- 555 [11] H. Di Benedetto, C. Sauzeat, K. Bilodeau, M. Buannic, S. Mangiafico, Q.T.  
556 Nguyen, S. Pouget, N. Tapsoba, J. Van Rompu, General overview of the time-  
557 temperature superposition principle validity for materials containing bituminous  
558 binder, *Int. J. Roads Airports.* 1 (2011) 35–52.
- 559 [12] Y. Ruan, R.R. Davison, C.J. Glover, The effect of long-term oxidation on the  
560 rheological properties of polymer modified asphalts, *Fuel.* 82 (2003) 1763–1773.  
561 doi:10.1016/S0016-2361(03)00144-3.

- 562 [13] F. Olard, H. Di Benedetto, A. Dony, J.-C. Vaniscote, Properties of bituminous  
563 mixtures at low temperatures and relations with binder characteristics, *Mater.*  
564 *Struct.* 38 (2005) 121–126. doi:10.1007/BF02480584.
- 565 [14] M.O. Marasteanu, A. Basu, S.A.M. Hesp, V. Voller, Time–Temperature  
566 Superposition and AASHTO MP1a Critical Temperature for Low-temperature  
567 Cracking, *Int. J. Pavement Eng.* 5 (2004) 31–38.  
568 doi:10.1080/10298430410001720792.
- 569 [15] A.F. Stock, *Alternative Modified Binders for Airfield Pavements*, Report no.  
570 AD-A197 902, 1988.
- 571 [16] L.-I. Palade, P. Attané, S. Camaro, Linear viscoelastic behavior of asphalt and  
572 asphalt based mastic, *Rheol. Acta.* 39 (2000) 180–190.  
573 doi:10.1007/s003970050018.
- 574 [17] C.W. Schwartz, N. Gibson, R.A. Schapery, Time-Temperature Superposition of  
575 Asphalt Concrete at Large Compressive Strains, *Transp. Res. Rec. J. Transp.*  
576 *Res. Board.* 1789 (2002) 101–112.
- 577 [18] C.W. Schwartz, N.H. Gibson, R.A. Schapery, M.W. Witczak, Viscoplasticity  
578 Modeling of Asphalt Concrete Behavior, in: *Recent Adv. Mater. Charact. Model.*  
579 *Pavement Syst.*, American Society of Civil Engineers, Reston, VA, 2003: pp.  
580 144–159. doi:10.1061/40709(257)10.
- 581 [19] Y. Zhao, Y. Kim, Time-Temperature Superposition for Asphalt Mixtures with  
582 Growing Damage and Permanent Deformation in Compression, *Transp. Res.*  
583 *Rec. J. Transp. Res. Board.* 1832 (2003) 161–172. doi:10.3141/1832-20.

- 584 [20] N.I.M. Yusoff, M.T. Shaw, G.D. Airey, Modelling the linear viscoelastic  
585 rheological properties of bituminous binders, *Constr. Build. Mater.* 25 (2011)  
586 2171–2189. doi:10.1016/j.conbuildmat.2010.11.086.
- 587 [21] M. Jaczewski, J. Judycki, Effects of deviations from thermo-rheologically simple  
588 behavior of asphalt mixes in creep on developing of master curves of their  
589 stiffness modulus, in: 9th Int. Conf. “Environmental Eng. 2014,” Vilnius  
590 Gediminas Technical University Press “Technika” 2014, Vilnius, Lithuania,  
591 2014. doi:10.3846/enviro.2014.157.
- 592 [22] M. Jaczewski, J. Judycki, P. Jaskuła, Modelling of Asphalt Mixes under Long  
593 Time Creep at Low Temperatures, in: *Transp. Res. Procedia*, 2016: pp. 3527 –  
594 3535. doi:10.1016/j.trpro.2016.05.323.
- 595 [23] M. Jaczewski, Wpływ zastosowania betonu asfaltowego o wysokim module  
596 sztywności na spękania niskotemperaturowe nawierzchni, Gdansk University of  
597 Technology, 2016.
- 598 [24] J. Judycki, Verification of the new viscoelastic method of thermal stress  
599 calculation in asphalt layers of pavements, *Int. J. Pavement Eng.* (2016) 1–13.  
600 doi:10.1080/10298436.2016.1199883.
- 601 [25] J. Sohm, T. Gabet, P. Horny, J.-M. Piau, H. Di Benedetto, Creep tests on  
602 bituminous mixtures and modelling, *Road Mater. Pavement Des.* 13 (2012) 832–  
603 849. doi:10.1080/14680629.2012.735795.
- 604 [26] N.W. Tschoegl, *The Phenomenological Theory of Linear Viscoelastic Behavior*,  
605 Springer Berlin Heidelberg, Berlin, Heidelberg, 1989. doi:10.1007/978-3-642-  
606 73602-5.





- 607 [27] F. Olard, H. Di Benedetto, General “2S2P1D” Model and Relation Between the  
608 Linear Viscoelastic Behaviours of Bituminous Binders and Mixes, *Road Mater.*  
609 *Pavement Des.* 4 (2003) 185–224. doi:10.1080/14680629.2003.9689946.
- 610 [28] J. Judycki, Analysis of selected rheological properties of asphalt concrete  
611 subjected to static load (in Polish), Gdansk University of Technology, 1975.
- 612 [29] J. Judycki, Non-linear viscoelastic behaviour of conventional and modified  
613 asphaltic concrete under creep, *Mater. Struct.* 25 (1992) 95–101.
- 614 [30] Y.R. Kim, Y.C. Lee, H.J. Lee, Correspondence Principle for Characterization of  
615 Asphalt Concrete, *J. Mater. Civ. Eng.* 7 (1995) 59–68. doi:10.1061/(ASCE)0899-  
616 1561(1995)7:1(59).
- 617 [31] C.Y. Cheung, D. Cebon, Experimental study of pure bitumens in tension,  
618 compression, and shear, *J. Rheol. (N. Y. N. Y.)* 41 (1997) 45–74.  
619 doi:10.1122/1.550858.
- 620 [32] H. Soenen, J. De Visscher, T. Tanghe, A. Vanelstraete, P. Redelius, R. Davis, R.  
621 Kluttz, M. Dunning, K. Chatti, Selection of binder performance indicators for  
622 asphalt rutting based on triaxial and wheel tracking tests, *J. Assoc. Asph. Paving*  
623 *Technol.* 75 (2006) 165–202.
- 624 [33] P. Des Croix, H. Di Benedetto, Binder-mix rheology: Limits of linear domain,  
625 non linear behaviour, in: *Proceeding Euroasphalt Eurobitume Congr. Strasbourg,*  
626 *Fr. 7-10 May, 1996.*
- 627 [34] J. Judycki, A new viscoelastic method of calculation of low-temperature thermal  
628 stresses in asphalt layers of pavements, *Int. J. Pavement Eng.* 19 (2018) 24–36.

- 629 doi:10.1080/10298436.2016.1149840.
- 630 [35] J. Skrzypek, Plasticity and creep, theory, application, excercises (in Polish),  
631 PWN, Warsaw, 1986.
- 632 [36] G.M. Rowe, M.J. Sharrock, M.G. Bouldin, R.N. Dongre, Advanced Techniques  
633 to Develop Asphalt Master Curves from the Bending Beam Rheometer, *Pet.*  
634 *Coal.* 43 (2001) 54–59.
- 635 [37] M. Williams, R.F. Landel, J.D. Ferry, The Temperature Dependance of  
636 Relaxation Mechanisms in Amorphous Polymers and Other Glass-forming  
637 Liquids, *J. Am. Chem. Soc.* 77 (1955) 3701–3707.
- 638 [38] G.M. Rowe, M.J. Sharrock, Alternate Shift Factor Relationship for Describing  
639 the Temperature Dependency of the Visco-Elastic Behaviour of Asphalt  
640 Materials, *Transp. Res. Rec. J. Transp. Res. Board.* 2207 (2011) 125–135.
- 641 [39] D.W. Christensen, D.A. Anderson, Interpretation of Dynamic Mechanical Test  
642 Data for Paving Grade Asphalt Cements, *J. Assoc. Asph. Paving Technol.* 61  
643 (1992) 68–116.
- 644 [40] Guide for Mechanistic-Empirical Design of New and Rehabilitated Pavement  
645 Structures, Final Report, Part 3 – Design and Analysis, 2004.
- 646 [41] D.W. Christensen, T. Pellinen, R.F. Bonaquist, Hirsh Model for Estimating the  
647 Modulus of Asphalt Concrete, *J. Assoc. Asph. Paving Technol.* 72 (2003) 121 –  
648 151.
- 649 [42] T. Pellinen, A. Zofka, M. Marasteanu, N. Funk, Asphalt Mixture Stiffness  
650 Predictive Models, *J. Assoc. Asph. Paving Technol.* 76 (2007) 575–625.



- 651 [43] M.O. Marasteanu, D.A. Anderson, Improved Model for Bitumens Rheological  
652 Characterization, in: Eurobitume Work. Performance-Related Prop. Bitum. Bind.,  
653 Luxembourg, 1999: p. Paper No. 133.
- 654 [44] M. Cholewińska, M. Iwański, G. Mazurek, The Impact of Ageing on the Bitumen  
655 Stiffness Modulus Using the CAM Model, *Balt. J. Road Bridg. Eng.* 13 (2018)  
656 34–39. doi:10.3846/bjrbe.2018.386.
- 657 [45] Refining the Simple Performance Tester for Use in Routine Practice,  
658 Washington, D.C., 2008.
- 659 [46] M. Pszczoła, J. Judycki, Testing of low temperature behaviour of asphalt  
660 mixtures in bending creep test, in: 7th Int. RILEM Symp. Adv. Test. Charact.  
661 Bitum. Mater. Adv. Test. Charact. Bitum. Mater., Rhodes, 2009: pp. 303–312.
- 662 [47] M. Pszczoła, M. Jaczewski, D. Rys, P. Jaskula, C. Szydłowski, Evaluation of  
663 Asphalt Mixture Low-Temperature Performance in Bending Beam Creep Test,  
664 *Materials (Basel)*. 11 (2018) 100. doi:10.3390/ma11010100.
- 665 [48] D.A. Anderson, D.W. Christensen, H.U. Bahia, R. Dongre, M.G. Sharma, C.E.  
666 Antle, Binder characterization and evaluation. In: Physical characterization, vol.  
667 3. Publication SHRP-A-369, Washington D.C., 1994.
- 668 [49] D.A. Anderson, M.O. Marasteanu, Physical hardening of asphalt binders relative  
669 to their glass transition temperature, *Transp. Res. Rec. J. Transp. Res. Board.*  
670 1661 (1999) 27–34.
- 671 [50] X. Lu, U. Isacsson, Laboratory study on the low temperature physical hardening  
672 of conventional and polymer modified bitumens, *Constr. Build. Mater.* 14 (2000)

- 673 79–88.
- 674 [51] S.A.M. Hesp, S. Iliuta, J.W. Shirokoff, Reversible aging in asphalt binders,  
675 Energy Fuel. 21 (2007) 1112–1121.
- 676 [52] J. Judycki, Influence of low-temperature physical hardening on stiffness and  
677 tensile strength of asphalt concrete and stone mastic asphalt, Constr. Build.  
678 Mater. 61 (2014) 191–199. doi:10.1016/j.conbuildmat.2014.03.011.
- 679 [53] J. Judycki, Bending test of asphaltic mixtures under statical loading, in: Proc.  
680 Fourth Int. RILEM Symp. Mech. Tests Bitum. Mix. Charact. Des. Qual. Control,  
681 Budapest, 1990: pp. 207–227.
- 682 [54] M. Pszczoła, J. Judycki, Comparison of calculated and measured thermal stresses  
683 in asphalt concrete, Balt. J. ROAD Bridg. Eng. 10 (2015) 39–45.  
684 doi:10.3846/bjrbe.2015.05.
- 685 [55] R. Kleizienė, A. Vaitkus, D. Čygas, Influence of asphalt visco-elastic properties  
686 on flexible pavement performance, Balt. J. Road Bridg. Eng. 11 (2016) 313–323.  
687 doi:10.3846/bjrbe.2016.36.
- 688 [56] Ł. Mejłun, J. Judycki, B. Dołżycki, Comparison of Elastic and Viscoelastic  
689 Analysis of Asphalt Pavement at High Temperature, Procedia Eng. 172 (2017)  
690 746–753. doi:10.1016/j.proeng.2017.02.095.
- 691 [57] B. Świeczko-Żurek, P. Jaskuła, J.A. Ejsmont, A. Kędzierska, P. Czajkowski,  
692 Rolling resistance and tyre/road noise on rubberised asphalt pavement in Poland,  
693 Road Mater. Pavement Des. 18 (2017) 151–167.  
694 doi:10.1080/14680629.2016.1159245.



- 695 [58] AASHTO T 322-03 Standard Method of Test for Determining the Creep  
696 Compliance and Strength of Hot-Mix Asphalt (HMA) Using the Indirect Tensile  
697 Test Device, (n.d.) 2006.
- 698 [59] M.O. Marasteanu, R. Velasquez, A.C. Falchetto, A. Zofka, Development of a  
699 Simple Test to Determine the Low Temperature Creep Compliance of Asphalt  
700 Mixtures, Final Report for Highway IDEA Project 133, 2009.
- 701 [60] A. Zofka, M. Marasteanu, M. Turos, Investigation of Asphalt Mixture Creep  
702 Compliance at Low Temperatures, Road Mater. Pavement Des. 9 (2008) 269–  
703 285. doi:10.1080/14680629.2008.9690169.
- 704 [61] A. Zofka, M. Marasteanu, M. Turos, Determination of Asphalt Mixture Creep  
705 Compliance at Low Temperatures by Using Thin Beam Specimens, Transp. Res.  
706 Rec. J. Transp. Res. Board. 2057 (2008) 134–139. doi:10.3141/2057-16.
- 707 [62] R. Velasquez, M. Marasteanu, J. Labuz, M. Turos, Evaluation of Bending Beam  
708 Rheometer for Characterization of Asphalt Mixtures, J. Assoc. Asph. Paving  
709 Technol. 79 (2010) 295–324.
- 710 [63] R. Velasquez, A. Zofka, M. Turos, M.O. Marasteanu, Bending beam rheometer  
711 testing of asphalt mixtures, Int. J. Pavement Eng. 12 (2011) 461–474.  
712 doi:10.1080/10298430903289956.
- 713 [64] M. Pszczoła, M. Jaczewski, C. Szydłowski, J. Judycki, B. Dołżycki, Evaluation  
714 of Low Temperature Properties of Rubberized Asphalt Mixtures, Procedia Eng.  
715 172 (2017) 897–904. doi:10.1016/j.proeng.2017.02.098.
- 716